Multi-temporal Monitoring for Road Slope Collapse by Means of LUTAN-1 SAR Data and High Resolution Optical Data

Xiang Zhang, Xinming Tang, Tao Li, Xiaoqing Zhou, Haifeng Hu, Xuefei Zhang, Jing Lu

Land Satellite Remote Sensing Application Center, Ministry of Natural Resources of P.R. China

Keywords: Slope Collapse, Lutan-1, Multi-temporal monitoring, DInSAR, Gaofen-2, Gaofen-7

Abstract

Collapse is one of the most destructive natural disaster, being sudden, frequent, and highly concealed, causing large-scale damage. On August 10, 2023, the slope of 108 national highway in Weinan, Shaanxi Province collapsed. The lower edge of the collapse slope body is the Luohe river, and the collapse body rushes into the river to form a barrier lake. Remote sensing technique can provide multiple dimensional information for disaster emergency and management. Lutan-1 SAR satellites are the first group L-band SAR constellation for multiple applications in China. Owing to the precise orbit control ability and high revisit characteristics for Lutan-1 SAR satellites, surface deformation monitoring with centimeter even millimeter accuracy may be achieved. Based on the multi-temporal pre-disaster and post-disaster Lutan-1 SAR data and high resolution optical data, the collapse information including the pre-disaster and post-disaster were extracted and analysed. From July 11 to 27, 2023, the pre-collapse deformation was obtained with the maximum value of 6 cm, and obvious deformation occurred before the collapse. Lutan-1 monitored results pre-collapse can provide certain information for disaster early identification. From July 27 to August 24, 2023, due to the serious incoherence caused by large deformation and ground changes, effective deformation information cannot be obtained based on the InSAR technique. In addition, the collapse information was clearly extracted by the high resolution optical data acquired pre-collapse and post collapse. After the collapse, significant deformation was extracted from August 24 to September 21 with the maximum value of 6 cm, indicating that obvious deformation still occurred over the collapse area. Through the analysis for the series results obtained by SAR and optical data, it is favourable for disaster emergency and management.

1. Introduction

Slope instabilities, especially along transportation corridors in mountainous areas, pose a threat to facilities, settlements and life (Martino et al. 2019). In mountainous areas, landslides is one of the most destructive natural disaster, being sudden, frequent, and highly concealed, causing large-scale damage (Huang 2012), and posing a threat to human life and infrastructure. Therefore, the study of the spatial and temporal evolution mechanism of landslides is particularly important. Only based on a clear understanding of the mechanism of landslides can the monitoring and prevention of landslides highlight their relevance, practicality, and purposefulness (Cenni et al. 2021). The continuous monitoring of deformation provides the key information to understand the spatial and temporal evolution mechanism of landslides and is one of the main methods for the early warning and prediction of landslides (Eberhardt et al. 2008).

Traditional geotechnical investigation and field monitoring techniques are the main ways to obtain landslide information. Surveys such as drilling, fixed non-prism monitoring, global navigation satellite system (GNSS) monitoring, and multi-point deep displacement monitoring can obtain detailed and accurate information of the surface and subsurface of landslides (Sun et al. 2019). In addition to these non-permanent site monitoring methods, optical imagery has become more widely used in the disaster field with the development of spaceborne and airborne technologies in the past decade. High-resolution spaceborne synthetic aperture radar (SAR) images can also realize surface deformation monitoring, which has all-day and multi-temporal characteristics. Interferometric synthetic aperture radar (InSAR) technology is not only used for the early identification of landslides (Bulmer et al 2006; Zhao et al. 2012), but also for landslide deformation monitoring (Xia et al. 2004).

On August 10, 2023, slope collapse occurred in Pucheng section of 108 National Highway in Weinan City, Shaanxi Province in China. The Land Satellite Remote Sensing Application Center of the Ministry of Natural Resources conducted pre-disaster deformation monitoring of the collapse area by using L-SAR satellite images. The collapse area in Weinan, Shaanxi Province had a shape variable of more than 6 cm within 16 days. According to the preliminary judgment of internal industry, there had been a short-term obvious deformation before the collapse. The west side was adjacent to the 108 National Highway, and the collapse caused the interruption of the road. The collapse area is located at the 108 National highway K16+600 to K16+900, the collapse of the body about 200 meters long, about 400 meters wide, about 2.5 meters thick, the total square of about 200,000 square, the collapse caused by the quake lake about 200 meters long, about 4 meters wide

Figure 1. Collapse area of 108 national higeway.

Slope collapse generally results in obvious ground deformation. Traditional monitoring methods have a large workload and are susceptible to objective conditions. Interferometric synthetic aperture radar (InSAR) has the advantages of large scale and high frequency monitoring (Gabriel et al. 1989). Abundant of research have focused on the slope collapse monitoring using different SAR data (Cui et al. 2023; Zocchi et al. 2023). LuTan-1 SAR satellite is the first group L-band SAR constellation in China. The two satellites have been successfully launched 2022. Due to the precise orbit control ability and two satellites operating in a common reference orbit, the revisit cycle of two LuTan-1 SAR satellites was reduced to 4 days, and the orbital cube can controlled within 350m orbital tube, which provide the basis for interferometric applications with high temporal and spatial coherence (Ji et al., 2023; Zhang et al., 2023).

The pre-collapse Lutan-1 SAR data were acquired on July 11 and July 27, 2023. In accordance with the relevant emergency response requirements, Lutan-1 satellites were employed for emergency observation and strict regression shooting in the collapse area. On August 24, September 21 and October 19, the strict regression Lutan-1 data were acquired for emergency observation after the collapse. In addition, optical remote sensing data was also acquired for emergency observations. Multi-source remote sensing data provided the potential for fast observation and analysis for collapse emergency and management.

2. Study Area and Datasets

2.1 Study Area

The road slope collapse is located in Pucheng section of 108 National Highway in Weinan City, Shaanxi Province in China, shown as Figure 2. The collapse area is near the Luo River, due to the soil collapse the total square of about 200,000 square, which induced the Channel blockage. Earth poured into the Luo River and blocked its channel, forming a barrier lake with a reservoir of about 650,000 cubic meters. It poses a threat to the safety of life and property of people downstream.

Road slope stability monitoring is very important for road safety operation. In order to reduce the threat of slope collapse, the reliable monitoring for road slope is necessary and significant. InSAR technique provided an effective approach and strategy for frequently and timely monitoring for road slope. Multiple Lutan-1 SAR data are employed to monitoring the road slope collapse occurred on August 10, 2023 in Pucheng section of 108 National Highway in Weinan City, Shaanxi Province in China.

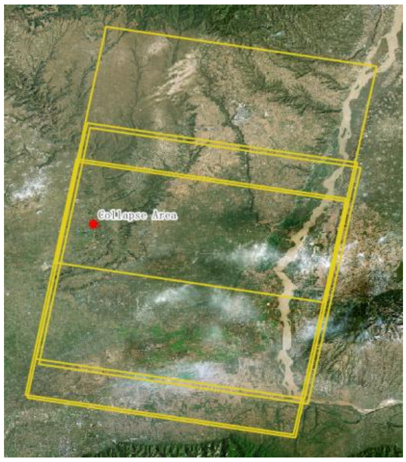

Figure 2. Study area and Lutan-1 covered area.

2.2 Datasets

On July 11and July 27, the Lutan-1 data were acquired before the road slop collapse. After the collapse, multi-temporal strict regression Lutan-1 SAR data were acquired for emergency observation. In addition, optical remote sensing data was also acquired for emergency observations.

Based on the pre-collapse and post-collapse Lutan-1 data, the whole slope collapse deformation was extracted in the first time, which is significant for disaster emergency and rescue. Furthermore, the deformation before and after the collapse were obtained for detailed analysis for the slope collapse.

The temporal baseline of Lutan-1 data was 16 days for pre-collapse analysis, the spatial baseline was 247.7 meters. The imaging mode was stripmap 1 with the nominal resolution 3 meters, shown as Figure 3. Detailed parameters of Lutan-1 data were shown in Table 1.

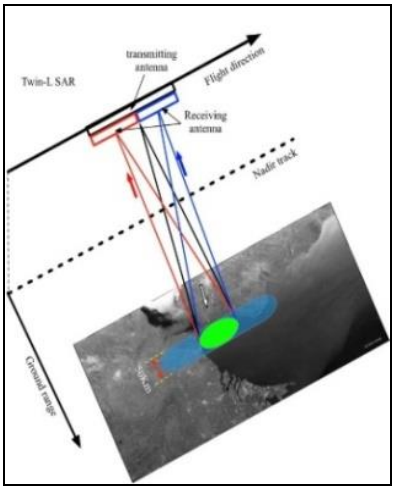

Figure 3. LuTan-1 SAR satellites stripmap1 imaging mode

Imaging Stage	Lutan-1 satellites	Acquisition time	Resolution	Polarization	Spatial Baseline	Temporal Baseline	Ascending/ Descending
Before the collapse	Lutan-1 A	11 July 2023	3 m	HH	247.7 m	16 Days	Descending
	Lutan-1 B	27 July 2023					
After the collapse	Lutan-1 A	24 August 2023			199.7 m	28 Days	
	Lutan-1 B	21 September 2023			319.9 m	28 Days	
	Lutan-1 A	19 October 2023			125.2 m	28 Days	

Table 1. Lutan-1 data for slope collapse deformation monitoring

https://doi.org/10.5194/isprs-archives-XLVIII-1-2024-867-2024

LandSAR software developed by Land Satellite Remote Sensing Application Center (LASAC) was applied for extracting the deformation field, including registration, resampling, interference, de-flattening and de-terrain phase, phase unwrapping and geocoding. In addition, the geometric correction and radiation optimization were applied for obtaining high geometric accuracy and radiation quality Lutan-1 SAR data. In combination with the corner reflectors data over calibration field, the azimuth and range error was derived to improve the geometric accuracy of Lutan-1 data. In order to solve the issue of L-band co-frequency interference, the co-frequency interference signal suppressed module developed by LASAC was employed to promote the Lutan-1 data radiation quality. Therefore, Lutan-1 data with accurate geometric and radiometric quality was obtained, which provided the potential for reliable deformation monitoring.

3. Results and Analysis

With the application of multiple optical and SAR satellites, multi-sources remote sensing data were acquired for disaster monitoring and analysis. Deformation monitoring information before the collapse and after the collapse were extracted and analysed.

3.1 Deformation monitoring before the collapse

The Lutan-1 SAR data acquired on July 11 and July 27 e were applied for the extraction of deformation before the collapse, and the results revealed that the obvious deformation occurred in the area pre-collapse with the maximum displacement of 6 cm. DInSAR processing results were shown as Figure 4.

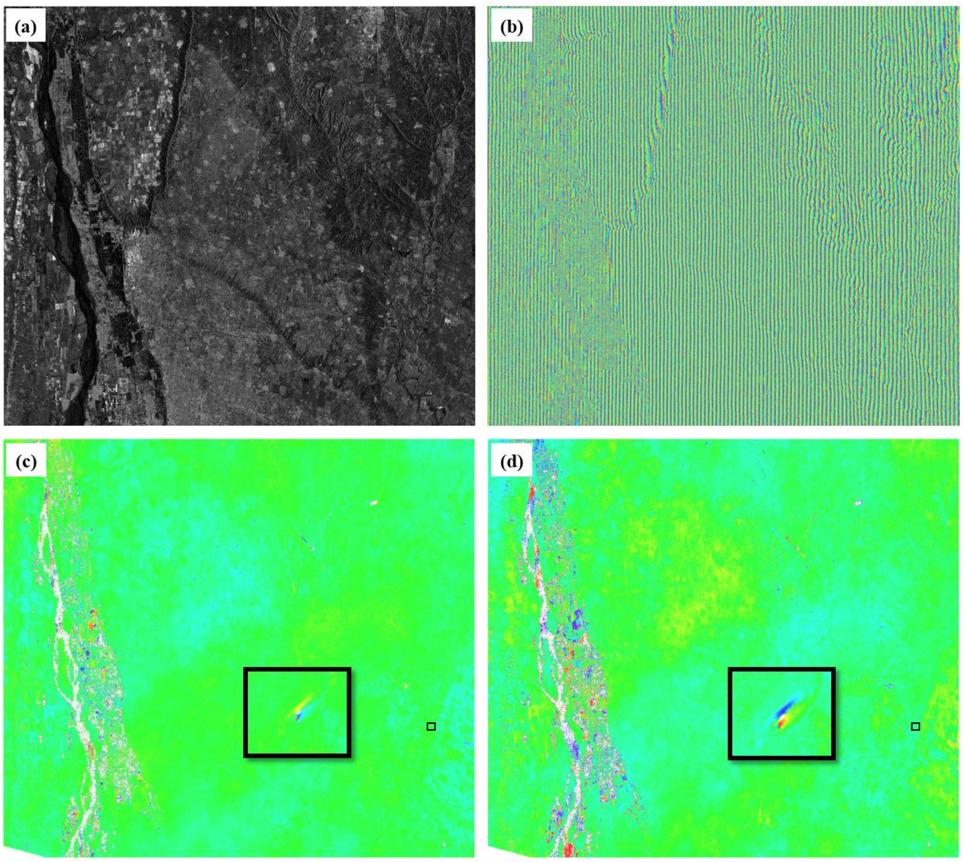

Figure 4. DInSAR processing results based on Lutan-1 data.
(a) Intensity diagram of the master image; (b) Interferogram; (c) Differential interferogram; (d) Unwrapped phase diagram

The coherence coefficient diagram before the collapse is shown as Figure 5. The average coherence of the interferogram is 0.88, which is due to the characteristics of L-band long wavelength and the advantages of Lutan-1 SAR satellites high precision orbit control. In addition, the coherence of the deformation center region is decreased due to large deformation, and the coherence of some regions is reduced to about 0.3.

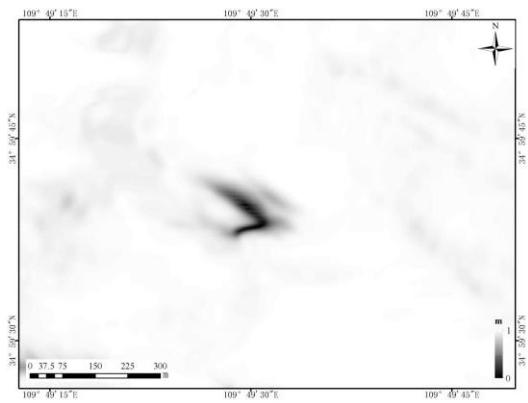

Figure 5. Coherence coefficient diagram from July 11 to July 27, 2023.

It can be seen from the deformation results that obvious deformation of the collapse area was extracted. The deformation of the collapse area before the collapse occurred was concentrated in the upper and lower part of the slope. The deformation of the upper part of the slope was mainly far from the radar line of sight, and the maximum cumulative subsidence within 16 days was more than -68mm, while the deformation of the lower part of the slope was mainly close to the SAR sensor, and the cumulative uplift can reach to 57mm.

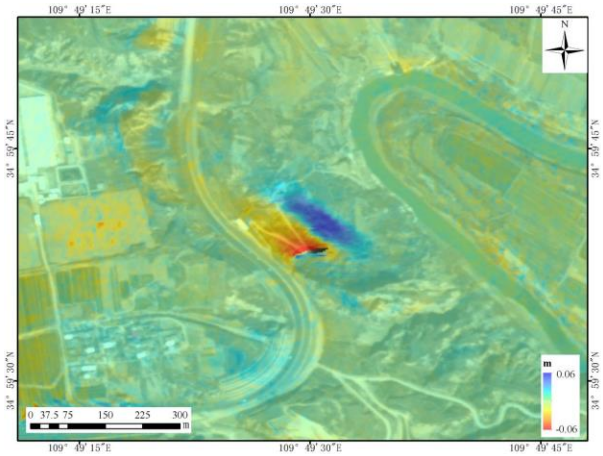

Figure 6. Pre-collapse deformation monitoring from July 11 to July 27 2023.

In general, the deformation results show that the top of the collapse body deforms and moves downward, and the downward accumulation leads to uplift in the lower part of the collapse body. Significant short-term deformation has occurred in this area before the collapse, which further validates the L-SAR satellite's ability to identify early hidden dangers of such geological disasters, and is expected to provide data support for pre-disaster prevention of geological disasters.

3.2 Analysis based on the Lutan-1 and optical data during the collapse

Multiple temporal Gaofen-7 and Gaofen-2 optical data with high spatial resolution was employed to analyse the road slope collapse. Before and after the collapse, there are obvious spectral characteristics variations over the disaster area, which can help us to identify the range and influence of collapse. The results indicated that the range of the collapse area was clearly characterized based on the high spatial resolution of Gaofen-7 and Gaofen-2 optic data, shown as Figure 7 and Figure 8.

The optical images of Gaofen-2 acquired on August 5, 2023 and August 15, 2023 are used to compare the changes before and after the collapse. It can be seen that the west side of the collapse area is close to the 108 National Highway, and the lower edge of the collapse slope body is the Luohe river, which interrupted the road, and the collapse body rushed into the river and caused a small dammed lake.

(a) Gaofen-2 acquired on August 5, 2023

(b) Gaofen-2 acquired on August 15, 2023

Figure 7. Gaofen-2 optical data before and after the collapse

In comparison with Gaofen-7 data before and after the collaspe, the obvious collapse area can be extracted. In addition, the road was diverted due to the collapse, and the construction of roads and infrastructure is also evident in the image acquired on Junaray 3, 2024.

(a) Gaofen-7 image acquired on March 14, 2023

https://doi.org/10.5194/isprs-archives-XLVIII-1-2024-867-2024 |

(b) Gaofen-7 image acquired on Junaray 3, 2024

Figure 8. Gaofen-7 optical data for collapse monitoring

In addition, coherence characterizes the variation degree of surface scattering characteristics. If the observed target change obviously between different periods, the coherence induced by SAR data will reduced significantly. Based on the above analysis, the collapse area may be characterized by the variation of coherence. Therefore, the coherence of the collapse area was analysed based on the Lutan-1 data, shown as Figure 9.

Due to the fact that the collapse will induce obvious ground variation, and thus the optical information change significantly between the pre-disaster and post-disaster images. Furthermore, through the interferometric analysis of the Lutan-1 SAR images before and after the collapse, it revealed the obvious coherence characteristics changes of ground objects in the collapse area, as shown in Figure 9. Therefore, the influence area of the collapse can be identified based on the coherence analysis using pre- and post- collapse Lutan-1 data. According to the coherence properties, the collapse area can be extracted from the coherence diagram, which provided an auxiliary indicator for disaster range identification.

As shown in Figure 9, the differential interference coherence coefficient of the two images before and after the collapse shows that due to the large deformation of the collapse, the coherence coefficient of the collapse area is low. It can also be seen from the deformation results in Figure 10 that due to the partial incoherence induced by the collapse, the effective deformation information before and after the collapse cannot be completely interpreted and obtained. However, the deformation trend of the collapse area can be mainly characterized.

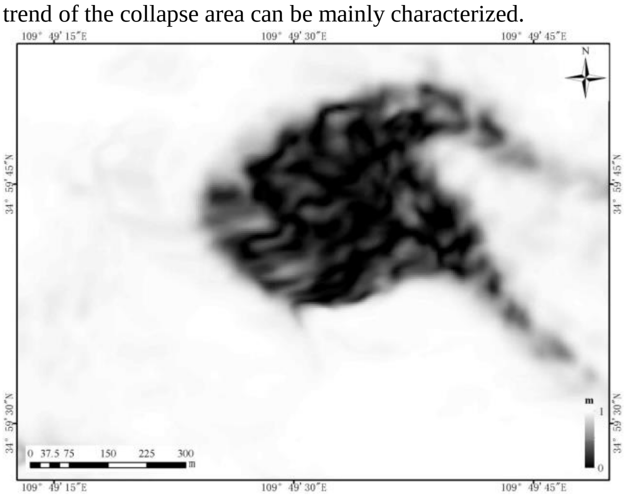

Figure 9. Coherence coefficient diagram from July 27 to August 24 2023.

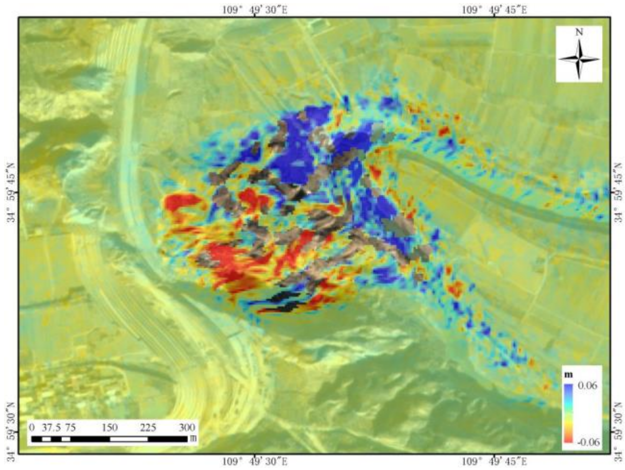

Figure 10. Pre-collapse and post-collapse deformation monitoring from July 27 to August 24 2023.

3.3 Post-collapse deformation monitoring analysis based on multi-temporal Lutan-1 data

(1) Deformation monitoring from August 24 to September 21 2023

Multi-temporal Lutan-1 data were applied for further deformation monitoring and analysis after the collapse. The Lutan-1 data acquired on August 24 and September 21 2023 were used to extract the deformation field over the collapse area.

As shown in Figure 7, it can be seen from the differential interference coherence coefficients of the two images one month after the collapse that the coherence coefficients within the collapse range are all greater than 0.5, and the overall coherence is good.

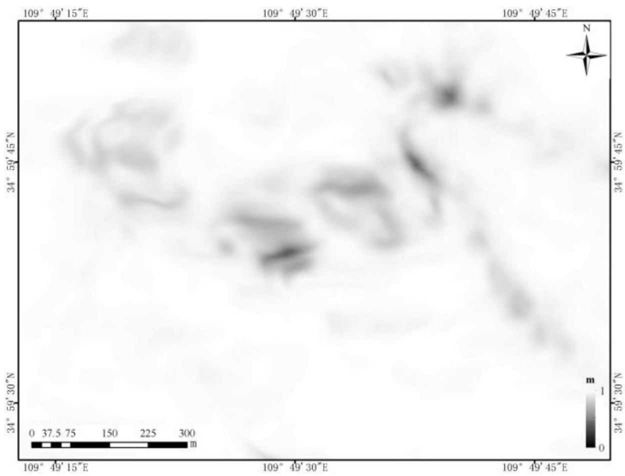

Figure 11. Coherence coefficient diagram from August 24 to September 21 2023.

From the deformation results of Figure 12, it can be seen that there is still significant deformation within the region one month after the collapse, and the deformation at the top of the slope is mainly near the radar line of sight. The maximum cumulative shape variable in 28 days is more than 56mm, and the deformation in the middle and lower part of the slope is mainly away from the radar line of sight, and the cumulative shape variable can reach -75mm.

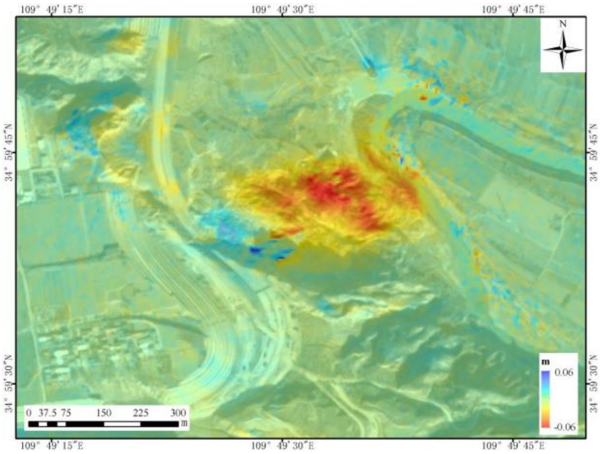

Figure 12. Post-collapse deformation monitoring from August 24 to September 21 2023.

(2) Deformation monitoring from September 21 to October 19 2023

The Lutan-1 data acquired on September 21 and October 19, 2023 were used to extract the deformation field over the collapse area. Figure 13 shows the differential interference coherence coefficient diagram of the two images two months after the collapse, the coherence coefficients within the collapse range are greater than 0.9, and the overall coherence is high owing to the accurate orbit control and high frequency observation.

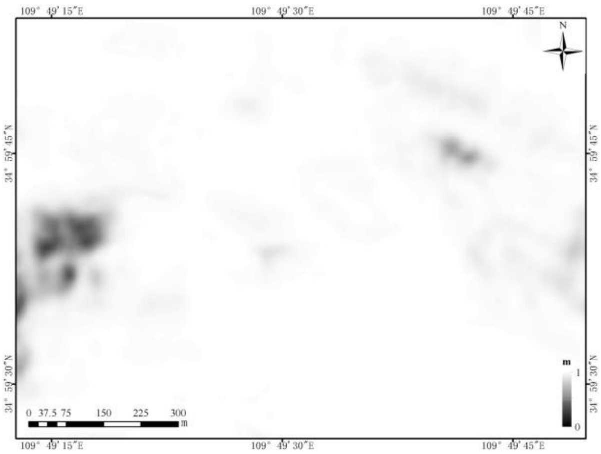

Figure 13. Coherence coefficient diagram from September 21 to October 19 2023.

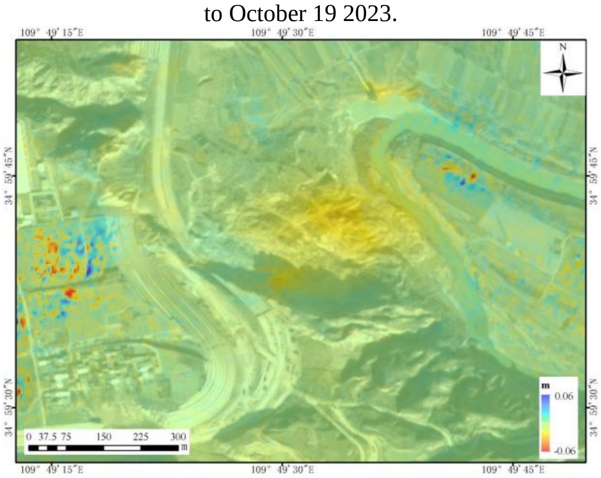

Figure 14. Post-collapse deformation monitoring from September 21 to October 19 2023.

As we can find from the deformation results in Figure 14, there are still small deformations over the collapse area two months after the collapse, which are located at the lower part of the slope far from the radar line of sight, and the cumulative deformation within 28 days reaches -26mm. The results show that with the accumulation of time, the soil is gradually compacted, the shape variable decreases, and the collapsed body tends to be stable.

4. Conclusions

Lutan-1 SAR satellite successfully acquired pre-collapse and post-collapse images, providing data support for the emergency response. The whole process monitoring of the road slope collapse is implemented by using multi-temporal Lutan-1 data, including deformation monitoring before and after collapse.

The results show that the slope deformation has occurred before the collapse, so the continuous monitoring in the early stage is expected to provide effective support for the early identification of the disaster.

The interference processing with Lutan-1 data before and after collapse cannot obtain effective deformation information because the collapse body changes significantly and the coherence deteriorate. The effective information of the collapse area is obtained by high resolution optical data before and after the collapse. In particular, the data of Gaofen-2 was acquired around the time of the accident collapse, which well characterized the collapse range. The data before and after the collapse of Gaofen-7 were also obtained. Due to the time interval, the surface changed obviously. Meanwhile, the construction situation of the national highway diverted due to the slope collapse was effectively monitored in Gaofen-7 data after the accident.

After the collapse, the Lutan-1 data obtained obvious deformation information of the collapse body. Due to soil gravity and water erosion, the collapse body was gradually compacted and obvious deformation occurred. From the significant deformation in the first month after the accident to the tiny deformation in the second month, it also indicates that the collapsed body gradually tends to be stable.

By monitoring the whole process of road slope collapse, the deformation monitoring ability of Lutan-1 SAR satellite data is effectively verified, and it also provides important data guarantee for the identification of hidden dangers in the early stage and disaster emergency response. The multi-source remote sensing technique provided the potential of disaster investigation, monitoring even early hidden danger identification.

Acknowledgements

This research was supported by the National Key R&D Programme of China (2023YFB3904905).

References

Bulmer, M.H., Petley, D.N., Murphy, W., Mantovani, F., 2006. Detecting slope deformation using two-pass differential interferometry: Implications for landslide studies on Earth and other planetary bodies. *J. Geophys. Res. 111*, E06S16.

Cenni, N., Fiaschi, S., Fabris, M., 2021. Integrated use of archival aerial photogrammetry, GNSS, and InSAR data for the monitoring of the Patigno landslide (Northern Apennines, Italy). *Landslides*, *18*, 2247–2263.

Cui, S., Wang, H., Pei, X., Luo, L., Zeng, B., Jiang, T., 2023. Research on Deformation Evolution of a Large Toppling Based on Comprehensive Remote Sensing Interpretation and Real-Time Monitoring. *Remote Sens. 15*, 5596.

Eberhardt, E., Watson, A.D., Loew, S., 2008. Improving the interpretation ofslopemonitoring and early warning data through better understanding of complex deep-seated landslide failure mechanisms. In *Landslides and Engineered Slopes: From the Past to the Future*, Taylor & Francis: London, UK, 39–51.

Gabriel, A.K., Goldstein, R.M., Zebker, H.A., 1989. Mapping small elevation changes over large areas: Differential radar inter-ferometry. *J. Geophys. Res. 94*, 9183–9191.

Huang, R., 2012. Mechanisms of large-scale landslides in China. *Bull. Eng. Geol. Environ. 71*, 161–170.

Ji, Y.N., Zhang, X., Li, T., et al., 2023: Mining Subsidence Monitoring Based on Lutan-1 Monostatic and Bistatic Data. *Remote Sens.*, 15, 5668.

Martino, S., Bozzano, F., Caporossi, P., 2019. Impact of landslides on transportation routes during the 2016–2017 Central Italy seismic sequence. *Landslides*, *16*, 1221–1241.

Sun, H., Wu, X., Wang, D., 2019. Analysis of deformation mechanism of landslide in complex geological conditions. *Bull. Eng. Geol. Environ. 78*, 4311–4323.

Xia, Y., Kaufmann, H., Guo, X.F., 2004. Landslide monitoring in the Three Gorges area using D-INSAR and corner reflectors. *Photogramm. Eng. Remote Sens. 70*, 1167–1172.

Zhao, C.Y., Lu, Z., Zhang, Q., Fuente, J.D.L., 2012. Large-area landslides detection and monitoring with ALOS/PALSAR imagery data over Northern California and Southern Oregon, USA. *Remote Sens. Environ. 124*, 348–359.

Zocchi, M., Kasaragod, A.K., Jenkins, A., 2023. Multi-Sensor and Multi-Scale Remote Sensing Approach for Assessing Slope Instability along Transportation Corridors Using Satellites and Uncrewed Aircraft Systems. *Remote Sens. 15*, 3016.

Zhang, X., Tang, X.M., Li, T., et al., 2023. Preliminary Assessment of Lutan-1 SAR Satellite for Multi-scale Mining Subsidence Monitoring. IGARSS, Pasadena California, 8166-8169.